ELSEVIER

Journal of Nuclear Materials 248 (1997) 412–417

journal of nuclear materials

Application of quantum beams to analysis of radioactive materials

M. Petri [a], L. Leibowitz [b], C.E. Johnson [b,*]

[a] *Fuels Engineering Division, Argonne National Laboratory, Argonne, IL 60439, USA*
[b] *Chemical Technology Division, Argonne National Laboratory, Argonne, IL 60439, USA*

Abstract

The methodology of quantum beams, an X-ray beam in this study, was used to examine the diffusion layer between a U–23 at.% Zr alloy and a Ni–16.4 at.% Cr alloy that exhibited nine distinct layers, many of which were mixtures of two phases. Four single-phase regions were less than 10 μm wide. A synchrotron X-ray beam, collimated by a 50 μm by 1 mm slit, was used to identify these phases. This beam was translated across the sample to obtain diffraction patterns throughout the diffusion zone. In this way, only a few phases were simultaneously within the beam, easing identification of the phases. Strains in the lattice due to solid solution were also observed. These microdiffraction techniques are applicable to a wide range of material systems. © 1997 Elsevier Science B.V.

1. Introduction

Understanding chemical interactions at the interface between dissimilar materials is a major concern for scientific and industrial applications. For example, to better understand the compatibility of metallic nuclear fuel and stainless steel cladding has been an important focus of research at Argonne National Laboratory [1,2]. During reactor operation, interdiffusion of fuel and cladding components can degrade the cladding over time by forming brittle intermetallic phases. Moreover, phases with relatively low melting temperatures may precipitate locally. To better understand the fuel/cladding interactions, detailed multicomponent isothermal interdiffusion experiments were performed on a binary U–23 at.% Zr alloy and a variety of Fe/Ni/Cr alloys [3]. In these early studies scanning electron microscopy (SEM) combined with energy dispersive X-ray analysis (EDX), was used to measure composition profiles across diffusion zones from which kinetic information was calculated. Intermetallic phase identification was not possible because crystal structures cannot be determined by SEM examination and conventional crystallographic techniques, such as X-ray diffraction, could not resolve the micron size phase layers in the diffusion zones. Furthermore, the use of transmission electron microscopy would involve formidable sample preparation difficulties with these easily oxidized, radioactive samples.

The present study employs a synchrotron source to extract structure and composition information from bonded materials that can lead to better understanding of the thermodynamic and kinetic processes involved. In contrast to scanning electron microscopy, synchrotron radiation sources can reveal both composition (via fluorescence) and structure (via absorption spectroscopy and diffraction), providing an ideal tool for studying materials and their interactions on a microscopic scale. Such experiments consist of bonding two materials under controlled conditions and examining the interdiffusion of the elements. In such a study, a collimated or focused synchrotron X-ray beam can be translated in steps across the diffusion zone. At each step, diffraction patterns or fluorescence spectra can be collected to provide structure and composition profiles along the diffusion path.

2. Experimental

To assess the feasibility of examining material interfaces using synchrotron sources, X-ray diffractometry of a fuel/cladding diffusion couple was carried out. Special precautions were taken to prevent the spread of radioactive contamination and to keep the reactive metallic fuel from

* Corresponding author. Tel.: +1-630 252 7533; fax: +1-630 252 4176; e-mail: johnsonce@cmt.anl.gov.

PII S0022-3115(97)00164-5

oxidizing. Although the binary U–Zr fuel alloy used unirradiated uranium, the sample was nonetheless radioactive. Furthermore, the metallic fuel readily oxidizes in air. Even thin oxide coatings could mask diffraction patterns from the underlying materials. In addition, significant oxidation of the surface could lead to flaking of a contaminated oxide. Future work is likely to include plutonium bearing or irradiated fuels, requiring additional precautions. To minimize these risks, a brass holder was designed to protect the sample surface from oxidation and to contain the radioactive materials. The design included a 100 μm thick Kapton window to enable viewing of the sample and allow X-rays to penetrate the holder.

Diffusion couples were made by stacking polished samples in a Kovar steel fixture. In this work a U–23Zr fuel alloy was mated with a Ni–16.4Cr alloy. The fixtured sample was sealed in an evacuated quartz tube and annealed for 4 h at 700°C in a horizontal tube furnace. After annealing, the quartz tube was allowed to cool in air outside the furnace. The fixtured sample was removed from the quartz tube cold-mounted in a self-setting resin, and cut longitudinally to expose a face parallel to the diffusion direction.

Beam collimation enabled narrow regions of the interdiffusion zone to be isolated so that diffraction patterns from only a few phases were collected simultaneously. The interdiffusion zone in the Ni–Cr/U–Zr couple was approximately 100 μm wide (Fig. 1) and contained nine distinct layers (Table 1). Five of those layers consisted of a mixture of two phases; four of the regions were less than 10 μm wide. An analysis of the composition profile across the diffusion zone revealed that U and Ni diffused faster

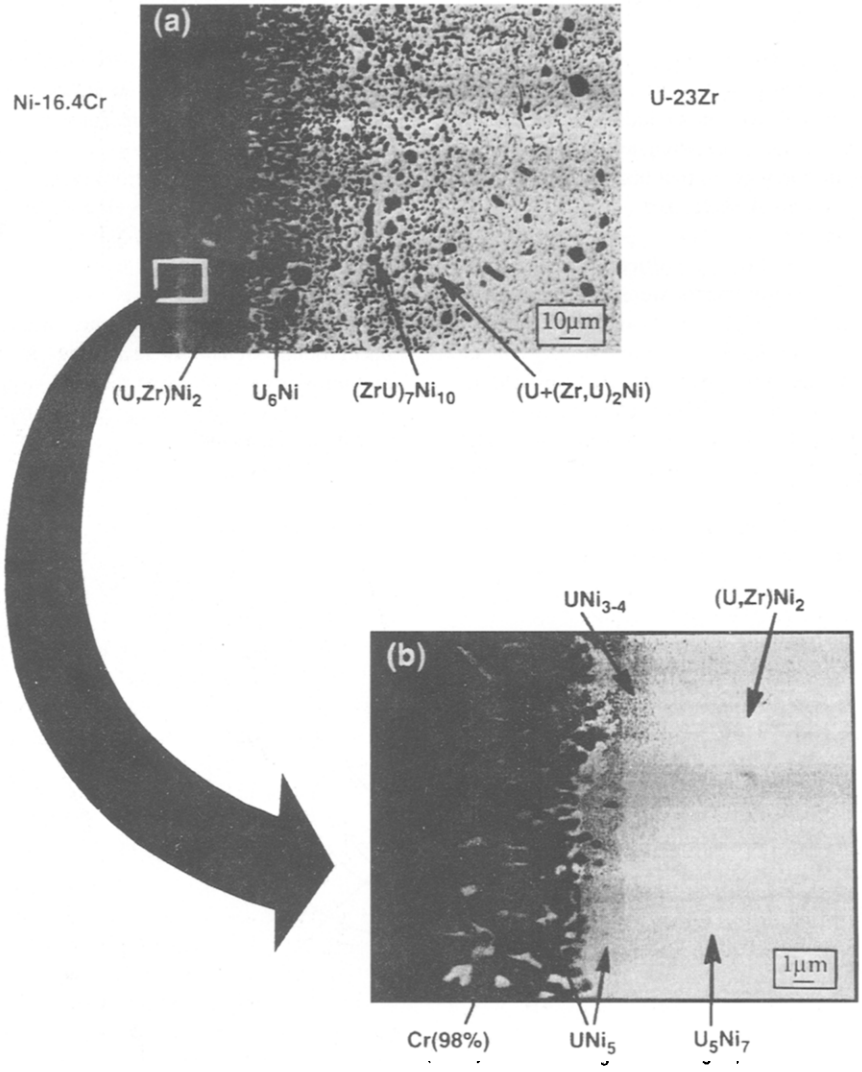

Fig. 1. SEM micrographs of the Ni–16.4Cr/U–23Zr diffusion couple after four days at 700°C. (a) Overall view of diffusion zone and (b) high-magnification view of diffusion zone edge near Ni–16.4Cr alloy [4].

Table 1
Phase layers in the Ni–Cr/U–Zr diffusion couple

Layer	Presumed Phases	Thickness (μm)
1 [a]	$Cr + UNi_5$	5
2 [a]	UNi_5	5
3 [a]	UNi_{3-4}	3
4 [a]	U_5Ni_7	4
5 [a,b]	$(U,Zr)Ni_2$	16
6 [a,b]	$(U,Zr)Ni_2 + U_6Ni$	14
7 [a,b]	$U_6Ni + (Zr,U)_7Ni_{10}$	15
8 [b]	$(Zr,U)_7Ni_{10} + U$	20
9 [b]	$(Zr,U)_2Ni + U$	25

[a] Phases contained in position 3 scan.
[b] Phases contained in position 2 scan.

than Zr, with effective penetration depths more than twice as large as that of Zr.

X-ray diffraction scans were performed on the synchrotron line X7A at the National Synchrotron Light Source (Brookhaven Lab.). This beam line includes a water-cooled channel cut, double crystal monochromator that produced a 1.2938 Å wavelength X-ray beam that had been collimated by a 1 mm by 1 mm slit. A motorized stage was used to translate the position of the slit with respect to the sample holder, which was mounted on a modified powder diffraction goniometer. All measurements were made in reflection geometry. A preliminary scan straddling the Ni–Cr/U–Zr interface, covering the 2θ range of 25° to 65° using an analyzer crystal in the scattered beam, showed the expected α-U pattern along with additional features associated with intermetallic phases in the diffusion zone. Crystallographic texture (preferred orientation) was observed in the α-U diffraction pattern. Normalizing the observed intensities to those expected for a random distribution of grains, the strongest component (3.4 times the average) was found to be near the (021) direction [4]. Contrary to our expectations, there was no clear evidence for the δ-UZr_2 phase. This may be due to the presence of oxygen or nitrogen impurities [5] or to the lack of cold work on the alloys [6].

Our analyses relied upon three compilations: Massalski's Binary Alloy Phase Diagrams [7] for binary systems, Villars and Calvert's Pearson's Handbook [8] for detailed crystallographic data, and the JCPDS-ICDD Powder Diffraction File [9] for d-spacings and relative intensities.

All subsequent patterns were collected using a 50 μm wide incident beam and a position sensitive detector (PSD) for increased data collection rates (Fig. 2). This detector had an effective range of 8° in 2θ. For each position within the diffusion zone, seven settings of the PSD were used centered on $2\theta = 32°$, 36°, 40°, 44°, 48°, 52°, and 56°. At each of these settings, counts were accumulated for 10 min. Identification of the intermetallic phases was typically based on patterns from the first two settings, which were richest in resolved diffraction lines.

As the scattering angles (θ and 2θ) were increased, the projected profile of the X-ray beam onto the sample changed. In particular, the length of the projection parallel to the phase boundaries was shortened at higher θ values. The most apparent consequence was a reduction in the background signal as scattering from the amorphous mounting resin — beyond the edge of the diffusion couple — was eliminated. Bragg scattering signals were not measurably affected.

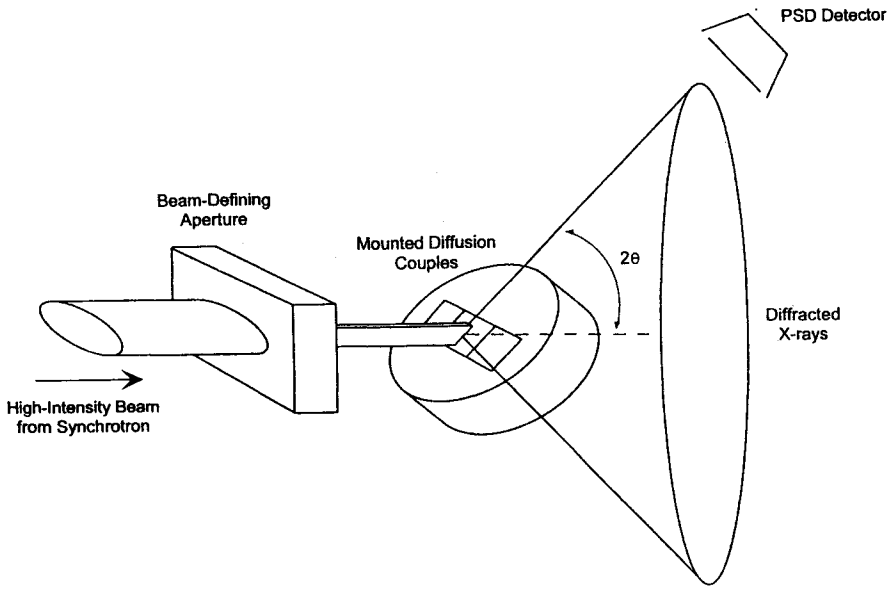

Fig. 2. Diffraction experiment geometry.

3. Results

Based on the analysis of the diffraction patterns, all the expected primary phases expected from the SEM results were confirmed (Table 1). The U–Ni and Zr–Ni binary systems are rich in stable intermetallic phases. Therefore, it was necessary to examine systematically the published diffraction and structural data to determine the existence of each possible phase in each diffraction pattern. Often there were no more than one to three uniquely defining peaks for a given phase. However, the combination of small beam dimension (and thereby small scattering volume) and excellent instrument resolution was sufficient to determine the existence of the pertinent phases. These studies confirmed the presence of the intermetallic phases predicted from the composition ratios measured by the SEM/EDX analyses, but with much less effort.

The diffraction patterns are shown in Figs. 3 and 4 for three different beam positions on the sample. Position 1 is

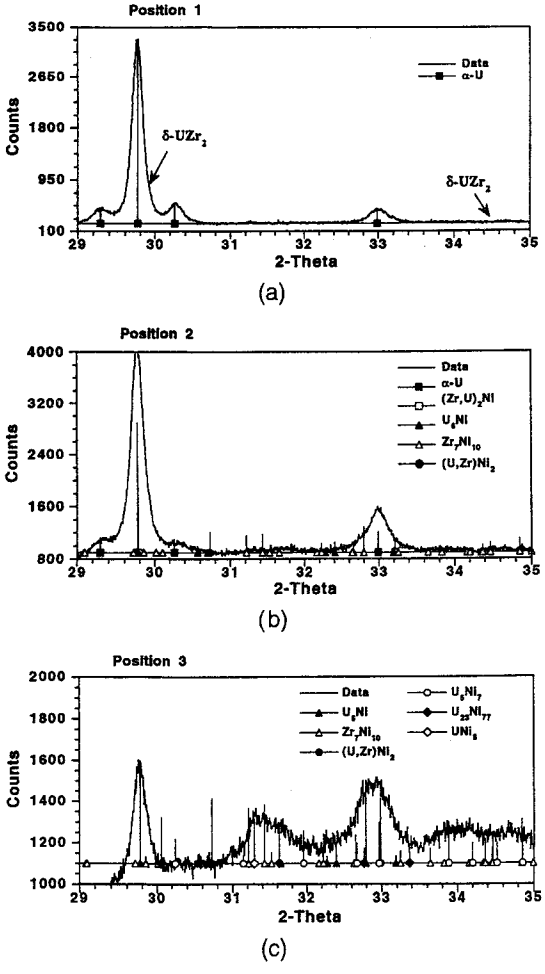

Fig. 3. Diffraction patterns from three beam position for 2θ from 29° to 35°.

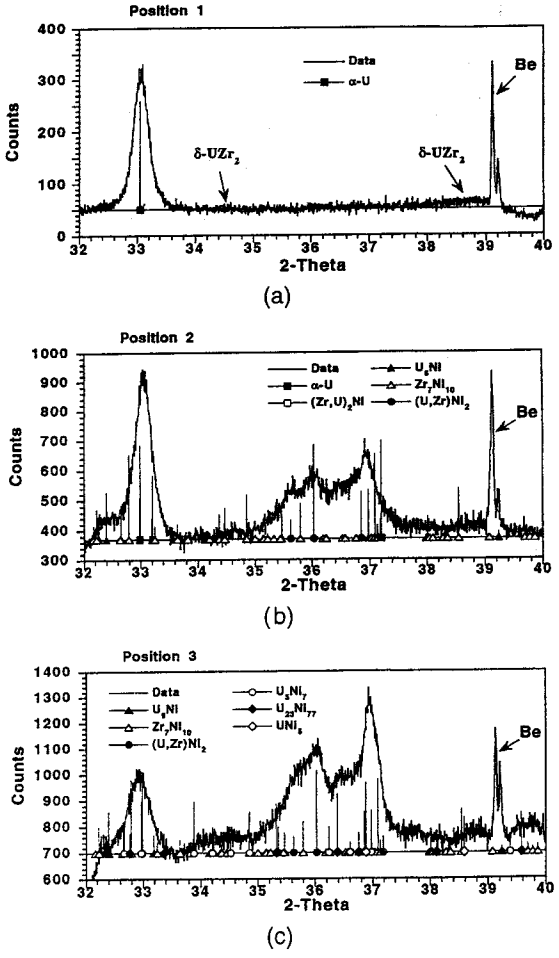

Fig. 4. Diffraction patterns from three beam position for 2θ from 32° to 40°.

in a region that is purely U–Zr, beyond the diffusion zone. Position 2 (300 μm away from position 1) includes portions of the diffusion zone, but overlaps the U–Zr alloy. Position 3 (340 μm away from position 1) lies entirely with in the diffusion zone near, but not in, the Ni–Cr alloy. Beyond this position the diffraction peak from pure Ni was observed.

4. Discussion

Of the two fuel components, U diffused more rapidly into the Ni–Cr cladding alloy. Moreover, aside from the high Cr phase in layer 1, Cr was not found in any of the intermetallic phases. Thus, the phases near the Ni–Cr alloy were dominated by U and Ni and are consistent with those predicted from the binary phase diagram. In contrast Zr–Ni compounds dominated near the fuel. The many possible phases between Zr and Ni, especially at high Zr concentra-

tions, suggest that the Zr–Ni compounds are more likely to form than the U–Ni compounds. Leibowitz et al. [10] have reported a positive deviation from Raoult's law for the U–Zr system, explaining why Zr and U segregate to different phases in layers 7, 8, and 9.

In the U–Zr/Ni–Cr diffusion couple, both planar and non-planar boundaries developed. Isothermal diffusion in a two component system invariably results in planar interfaces between phases. In the higher-order systems, however, there is an extra degree of freedom that allows composition changes along the interface. In this case, then, morphological instabilities of the interface are possible, leading to non-planar boundaries and eventually to multiphase regions. Whether perturbations along the interfaces along the interfaces will become unstable depends, among other things, on the competition between the high concentration gradients ahead of a perturbation (enhancing the instability) and the increased energy of a curved boundary (damping the instability). These effects are reflected in the diffusion path. If diffusion follows a tieline connecting two phases, the interface between the phases will be planar. Alternatively, if the path crosses tielines, non-planar boundaries may be possible. With non-planar interfaces and multiphase regions, distinguishing phases in a diffraction pattern becomes important, regardless of the size of the X-ray beam.

The sequence of phases from one end of the diffusion zone to the other generally follows a progression from high-U and high-Zr phases on the U–Zr side to low-U and low-Zr toward the Ni–Cr side. The (U, Zr)Ni_2 phase is a notable exception in that it occurs closer to the U–Zr end of the couple than the U_5Ni_7 phase even though it has a lower uranium content. On factor which may influence which phases appear and their sequence across the diffusion zone is the crystallographic similarity of the neighboring phases. This explanation is supported by the gradual progression of the diffraction peak intensities (Figs. 3 and 4) from the characteristic α-U peaks (the triplet centered at $2\theta = 33.0°$) to the (111) reflection of Ni at $2\theta = 37.0°$ (Fig. 5). The Be line seen in Fig. 4 is an artifact due to the presence of a beryllium window covering the sample when these diffraction patterns were collected.

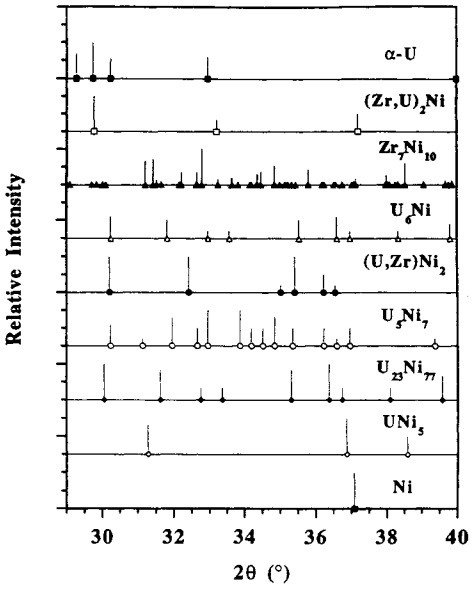

Fig. 5. Diffraction patterns for the phases confirmed in the Ni–16.4Cr/U–23Zr diffusion couple.

The SEM results were accurate in their assessment of intermetallic phases present. In the more complicated systems, however, SEM can be limited by the availability of published phase diagrams and crystal structures. On the other hand, X-ray diffraction does not inherently suffer from this limitation. With improved collimation or focusing of X-ray beams to reduce the problem to a few phases, structure determination of unknown phases becomes possible. Even though the diffraction patterns from an X-ray beam collimated to 50 μm verified the presence of the predicted phases. Figs. 3 and 4 clearly illustrate that some of the identifications are tenuous because of strong peak overlap from different phases. However, this problem is expected to be easily mitigated when X-ray beams of 10 μm or less, are used for the analysis.

5. Conclusions

This work defines a new direction for investigation of intermetallic diffusion in fuel cladding systems. By translating a finely collimated beam of X-rays through the diffusion zone of a U–Zr/Ni–Cr diffusion couple, the stepwise progression of intermetallic phases can be monitored. To improve the quality of the data future studies should tune the X-rays to a lower energy in order to improve the signal-to-noise ratio by eliminating fluorescence X-rays. In addition using a beamline with an insertion device (a wiggler or an undulator) or using focusing optics could increase the flux on the sample by two orders of magnitude or more. This same study could then be performed with a much smaller beam size. This would mean that only one or two phases would be analyzed simultaneously, greatly aiding phase identification. One can imagine examining the evolution of the diffraction pattern as, say, a 5 μm wide beam is translated across a diffusion zone.

References

[1] R.G. Pahl, D.L. Porter, C.E. Lamb, G.L. Hofman, Metall. Trans. 21A (1990) 1863.
[2] C.E. Till, Y.I. Chang, American Power Conference 48 (1986) 688.
[3] D.D. Keiser, M.A. Dayananda, J. Nucl. Mater. 200 (1993) 229.

[4] M.H. Mueller, J.W. Richardson, Jr., A.J. Schultz, F.K. Ross, D.G. Reichel, in: Proc. 8th Int. Conf. On Texture of Materials, (ICOTOM-8), ed. J.S. Kallend (1988), p. 209.
[5] F.A. Rough, A.E. Austin, A.A. Bauer, J.R. Doig, Battelle Memorial Institute Report BMI-1092, Columbus, OH, 1956.
[6] S.T. Zegler, Argonne National Laboratory Report, ANL-6055, Argonne, IL, 1962.
[7] T.B. Massalski, Binary Alloy Phase Diagrams, 2nd Ed. (ASM International, Materials Park, OH, 1990).
[8] P. Villars, L.D. Calvert, Pearsons Handbook of Crystallographic Data for Intermetallic Phases, 2nd Ed. (ASTM International, Newbury, OH, 1991).
[9] JCPDS International Centre for Diffraction Data, Powder Diffraction File Alphabetical Index (JCPDS-ICDD, Swarthmore, PA, 1992).
[10] L. Leibowitz, E. Veleckis, R.A. Blomquist, A.D. Pelton, J. Nucl. Mater. 154 (1988) 145.